

TRIUMF - EEC SUBMISSION EEC meeting: 202401S <i>Original Proposal</i>		Exp. No. S2373 - <i>Proposed</i>
		Date Submitted: 2023-12-15 05:36:17

Title of Experiment:

Lifetime of the key $^{30}\text{P}(\text{p},\gamma) ^{31}\text{S}$ resonance in novae

Spokesperson(s) for Group

B. Davids, L. J. Sun, C. Wrede

Safety Coordinator(s) for Group

B. Davids

Current Members of Group:

(name, institution, status)

B. Davids	TRIUMF/SFU	Research Scientist
L. J. Sun	MSU/FRIB	Research Associate
C. Wrede	MSU/FRIB	Professor
A. Adams	MSU/FRIB	Student (PhD)
C. Angus	University of York	Student (PhD)
A. Banerjee	SINP	Associate Professor
T. Budner	ANL	Research Associate
M.Y.H. Chan	Northwestern U.	Assistant Professor
J. Chen	MSU/FRIB	Research Scientist
J. Dopfer	MSU/FRIB	Student (PhD)
N. Esker	SJSU	Assistant Professor
M. Friedman	HUJI	Lecturer
C. Fry	LANL	Research Scientist
A.B. Garnsworthy	TRIUMF	Senior Research
G. Hackman	TRIUMF	Research Scientist
K. Hudson	SFU	Student (Graduate)
J. Jose	UPC	Professor

V. Karayonchev	TRIUMF	PDF
O.S. Kirsebom	Dalhousie U.	Research Scientist
L. Le	SJSU	Student (Graduate)
R. Mahajan	LSU/FSU	Research Associate
M. Oliver	SJSU	Student (Graduate)
C. Ruiz	TRIUMF	Research Scientist
R. Russell	University of Surrey	Student (PhD)
J. Surbrook	LANL	Research Associate
Ö. Sürer	Miami U.	Assistant Professor
V. Vedia	TRIUMF	PDF
L. Wagner	TRIUMF	PDF
L. Weghorn	MSU/FRIB	Student (PhD)
T. Wheeler	MSU/FRIB	Student (PhD)
J. Wilkinson	LLNL	Research Associate
E.J. Williams	TRIUMF	PDF
D. Yates	UBC	Student (PhD)

Beam Shift Requests:

21 shifts on: DSL (SEBT1)

Basic Information:

Date submitted: 2023-12-15 05:36:17

Summary: In classical novae, the radiative proton capture on the phosphorus-30 isotope acts as a nucleosynthesis bottleneck in the flow of material to heavier masses and subsequently influences many astronomical observables. The dominant uncertainty in the current estimates of this reaction rate is attributed to the unknown lifetime of the 260-keV resonance. We propose to measure the lifetime using the Doppler-shift attenuation method and will employ Markov chain Monte Carlo-based Bayesian statistical techniques for rigorous uncertainty quantification. The results of this experiment will be input to a state-of-the-art hydrodynamic nova model, allowing for comparisons between model predictions and astronomical observations, with minimal nuclear-related uncertainties.

Experimental Facility

ISAC Facility:

ISAC-II Facility: DSL (SEBT1)

Have all the Facility Coordinators and/or Collaboration spokespersons of the relevant experimental facilities been made aware of this proposal?: Yes

Secondary Beam

Isotope: 32S

Energy: 128 MeV

Optimal Intensity: 1.8e10

Minimum Intensity: 0.6e10

Maximum Intensity: 4.5e10

OLIS/ISAC: OLIS

Target/Source: Unknown

Energy Units: keV

Energy spread-maximum: Minimal

Time spread-maximum: Minimal

Angular Divergence: Minimal

Spot Size: 2

Charge Constraints:

Beam Purity: 100

Special Characteristics:

Safety Issues:

No major hazards. The beam current should be kept low enough that neutron radiation from the target does not become an issue. The 244Cm13C gamma source should be handled with care.

1 Abstract

In classical novae, the $^{30}\text{P}(p, \gamma)^{31}\text{S}$ reaction acts as a nucleosynthesis bottleneck in the flow of material to heavier masses affecting several observables. The dominant source of uncertainty in the current recommended reaction rate is the theoretical γ decay width of the $J^\pi = 3/2^+$, 259.81(29)-keV resonance at $E_x = 6390.46(16)$ keV in ^{31}S . We propose to measure the lifetime of the key ^{31}S resonance using the Doppler Shift Lifetimes 2 (DSL2) facility at TRIUMF. The ^{31}S excited states will be populated by the $^{3}\text{He}({}^{32}\text{S}, \alpha)^{31}\text{S}$ reaction. The deexcitation γ rays will be detected by a clover-type high-purity germanium detector in coincidence with the α particles detected by a silicon detector telescope. We will employ the Doppler-shift attenuation method and Markov chain Monte Carlo-based Bayesian statistical techniques to perform lineshape analyses of γ -ray data. Our primary objective is to establish the first experimental constraint on the lifetime, with rigorous uncertainty quantification. Combining the well-known energy, spin and parity, and proton-decay branching ratio of this resonance, we will be able to pin down the $^{30}\text{P}(p, \gamma)^{31}\text{S}$ reaction rate, enabling more accurate simulations of nova observables.

2 Scientific Value

Classical novae are among the most frequent thermonuclear stellar explosions in the Galaxy. They are powered by thermonuclear runaways occurring in the accreted envelope transferred from a companion star onto a compact white dwarf in a close binary system [1, 2]. The $^{30}\text{P}(p, \gamma)^{31}\text{S}$ reaction plays an important role in understanding the nucleosynthesis of $A \geq 30$ nuclides in oxygen-neon novae [3]. The uncertainty in the $^{30}\text{P}(p, \gamma)^{31}\text{S}$ rate impacts the nova observables, such as the $^{30}\text{Si}/{}^{28}\text{Si}$ isotopic abundance ratios useful for the identification of pre-solar nova grains [4], the O/S, S/Al, O/P, and P/Al abundance ratios that are good candidates for nova thermometers [5], and the Si/H abundance ratio, which can be used to constrain the degree of mixing between the white dwarf's outer layers and the accreted envelope [6]. It is not currently possible to measure the $^{30}\text{P}(p, \gamma)^{31}\text{S}$ reaction directly because intense low energy ^{30}P beams are not available. Through nuclear structure measurements, the thermonuclear rate of the $^{30}\text{P}(p, \gamma)^{31}\text{S}$ reaction over most of the peak nova temperatures (0.1–0.4 GK) has been found to be dominated by $\ell = 0$ proton capture into a 260-keV resonance [7, 8, 9] (Fig. 1). Recent experimental work has unambiguously determined the energy, the spin and parity, and the decay branching ratios of this resonance [8, 10, 11], leaving the lifetime as the largest remaining source of uncertainty in the resonance strength, as well as the last missing piece of experimental information for this state.

Until Feb 2023, only three relatively long-lived ^{31}S states at 1248 [12, 13, 14, 15], 2234 [12], and 4451 keV [15, 16] had reported lifetime measurements. In our experiment S1582 with the original Doppler Shift Lifetimes (DSL) facility at TRIUMF, we determined the lifetimes of the two long-lived ^{31}S states at 1248 and 2234 keV and obtained strong upper limits on the lifetimes of four short-lived states at 3076, 3435, 4971, and 5156 keV for the first time. We applied Markov chain Monte Carlo (MCMC) based Bayesian inference techniques to analyze γ -ray lineshapes acquired with the Doppler-shift attenuation method (DSAM) for the first time. We also observed evidence for γ rays originating from the astrophysically important $3/2^+$ resonance at 6390 keV, and the probability distribution obtained from Bayesian analysis suggests a lifetime below 20 fs. Shell model calculations using USD Hamiltonians predicted its lifetime to be 4.3 fs (USDA), 24 fs (USDB), 3.5 fs (USDC), 1.8 fs (USDE), 2.8 fs (USDI), and 1.3 fs (USDC-shifted) [17, 18, 19]. Based on the aforementioned studies, we can estimate that the lifetime falls within the femtosecond range, and therefore, the DSAM remains the most applicable approach. However, in order to establish stronger constraints on the lifetime, it is necessary to conduct a more sensitive measurement [18].

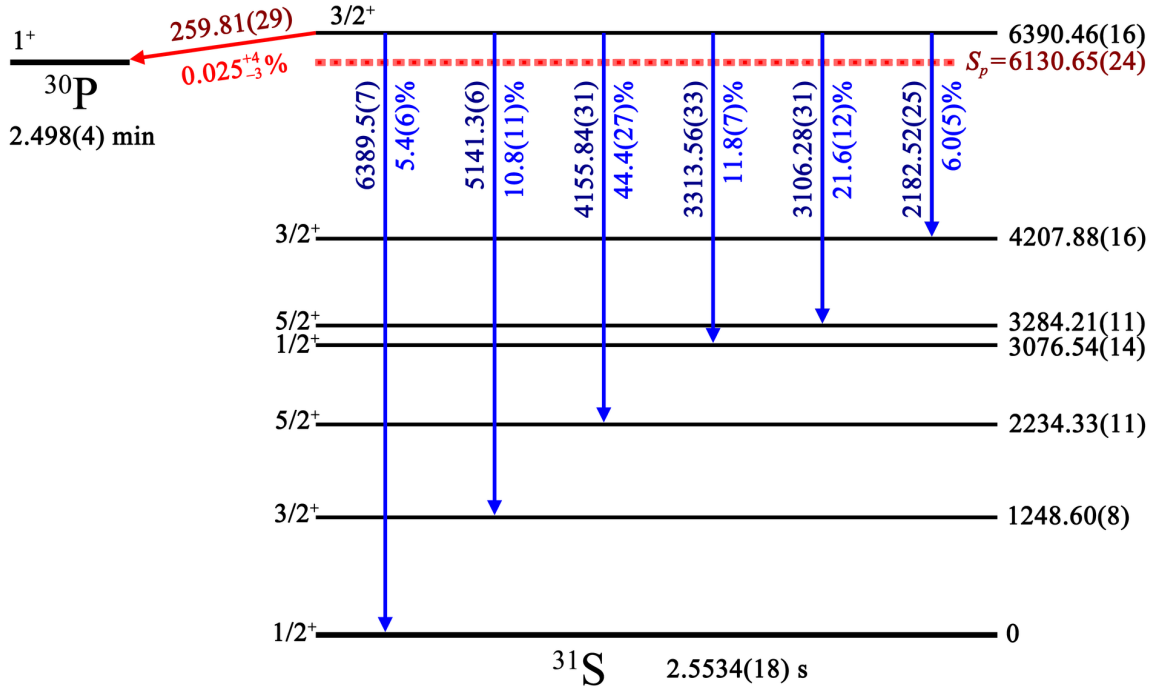


Figure 1: Known decay scheme of the $^{30}\text{P}(p, \gamma)^{31}\text{S}$ resonance at 6390 keV. The excitation energies and the proton separation energy are in units of keV and adopted from Ref. [9]. The transition energies and decay branching ratios are adopted from Refs. [8, 10, 11, 17].

3 Experimental Equipment

Motivated primarily by the unknown or imprecise lifetimes of excited states of astrophysical importance, we built the DSL facility at TRIUMF. As shown in Fig. 2, a scattering chamber was designed to provide a clean environment conducive to detecting γ ray emission from excited nuclear states populated in heavy ion-induced transfer reactions in inverse kinematics [20]. Reaction products gain more energy in inverse kinematics and lead to larger Doppler shifts in γ ray peaks, thereby improving the lifetime sensitivity of the DSAM.

Since its completion in 2005, the DSL setup has been used with $(^3\text{He}, \alpha)$ reactions to measure the lifetimes of ^{19}Ne states relevant to the $^{15}\text{O}(\alpha, \gamma)^{19}\text{Ne}$ reaction rate [21, 22], the lifetimes of ^{15}O states relevant to the $^{14}\text{N}(p, \gamma)^{15}\text{O}$ reaction rate [23], the lifetimes of ^{23}Mg states relevant to the $^{22}\text{Na}(p, \gamma)^{23}\text{Mg}$ reaction rate [24], and the lifetimes of ^{31}S states relevant to the $^{30}\text{P}(p, \gamma)^{31}\text{S}$ reaction [18, 25].

There are several factors that limit the sensitivity of the DSL lifetime measurements. We cannot significantly increase the ^{32}S beam intensity above the 10 pnA achieved in S1582 due to target heating. Also, we cannot increase the amount of ^3He implanted due to blistering of the Au substrate. As a result, our focus has been on improving the detection efficiency. In 2021, we upgraded the DSL facility to DSL2 by replacing the two ORTEC B Series silicon surface barrier detectors [26] with a 139 μm thick MICRON W1 double-sided silicon strip detector (DSSD) [27] and a 1011 μm thick MSX25 single-sided silicon detector [28] (Fig. 3). The surface area of the two ORTEC detectors was 150 mm^2 . Limited by the aperture in front of them, the telescope only covered 1.0% of the 4π solid angle. In contrast, the new telescope consists of larger detectors with an area of 2500 mm^2 and is able to cover approximately 34% of the 4π solid angle.

We have developed a detailed Monte Carlo simulation using GEANT4 [29, 30] to model the γ -ray lineshapes obtained by both DSL and DSL2 (Fig. 4). Based on our simulation results on the key ^{31}S resonance, the α

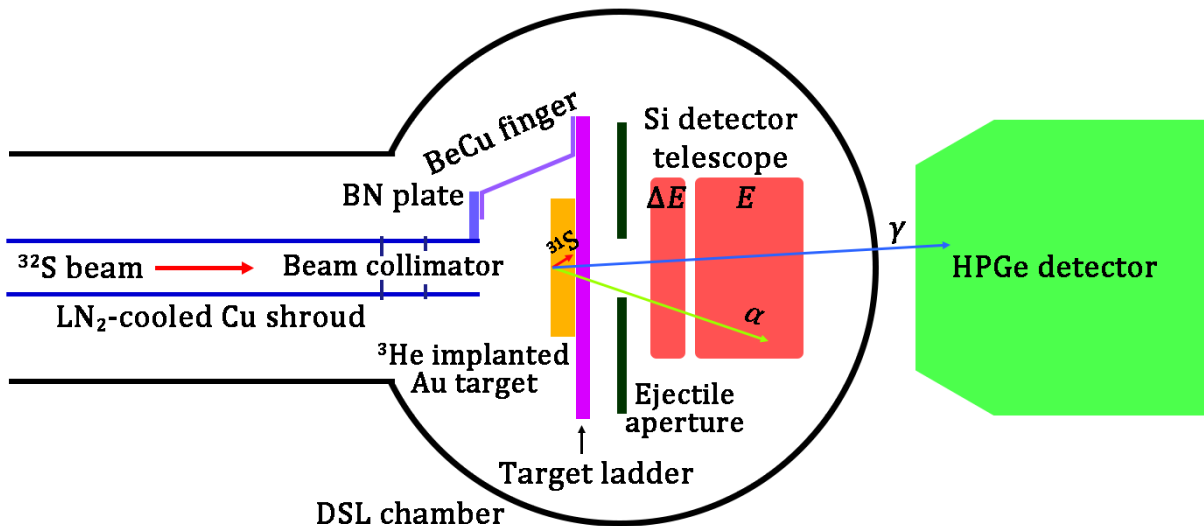


Figure 2: Schematic of the DSL experimental setup. The ejectile aperture has been removed in the DSL2 setup.

detection efficiency is increased by a factor 11 primarily due to the much higher solid angle coverage of the new Si telescope. The γ -ray detection efficiency is increased by a factor of 1.3. This improvement is attributed to the elimination of the collimator and detector mount, resulting in less attenuation of γ rays between the target and the Ge detector in DSL2. With the same amount of beam time, the overall statistics of the γ ray of interest at 4156 keV can be increased by a factor of 14, which will greatly benefit the sensitivity of lifetime measurements. Furthermore, the overall lineshape observed in DSL2 is subject to more kinematic broadening, but we can leverage the segmented feature of the DSSD to investigate lineshapes by selectively gating on α -particles in individual pixels.

The DSL2 setup has been successfully commissioned during the first run of S2193: Lifetime of the key $^{22}\text{Na}(p, \gamma)^{23}\text{Mg}$ resonance in novae, in December 2022 [31]. The data analysis is currently in progress, and a second run will be scheduled once the desired beam intensity of ^{24}Mg is achieved [32].

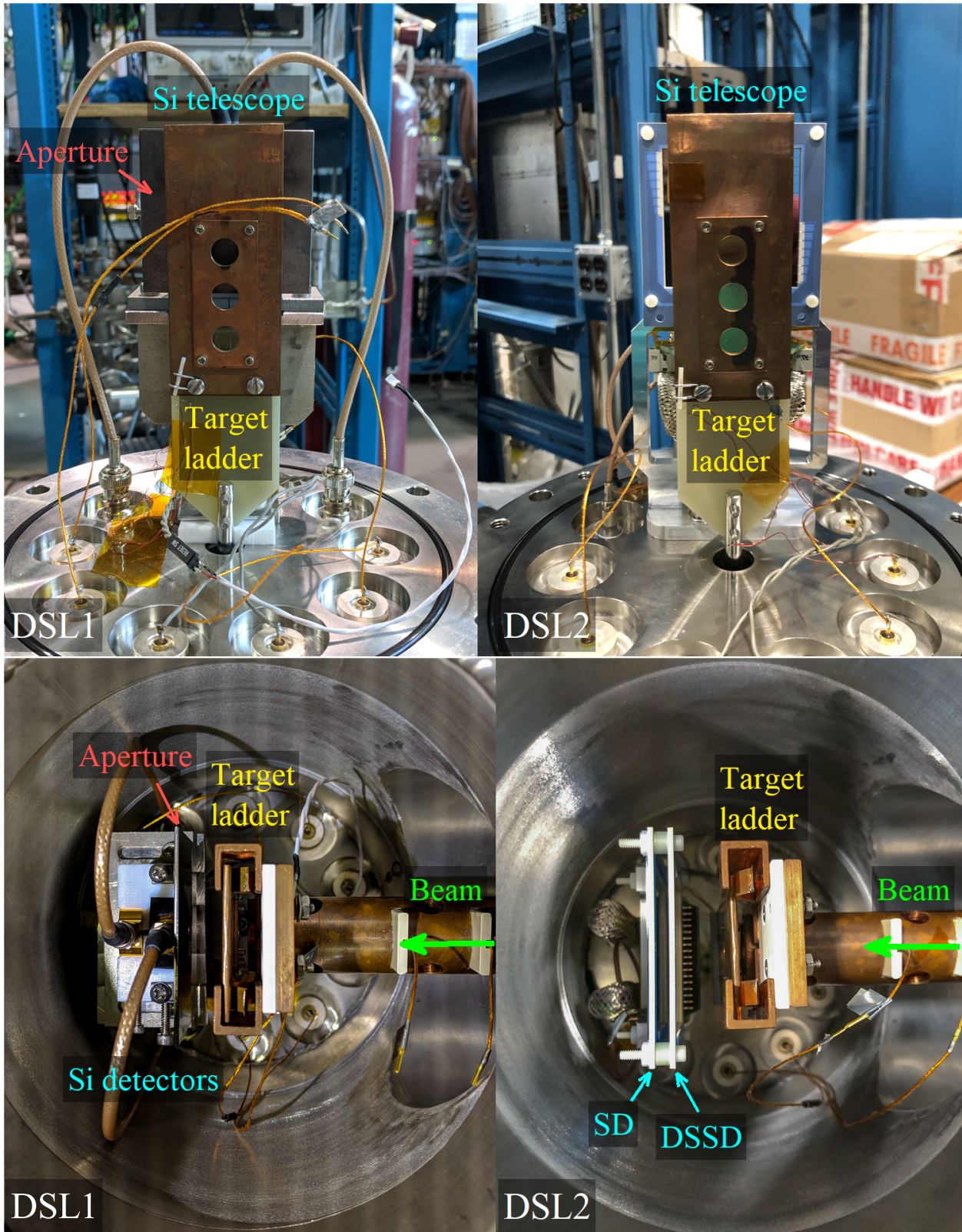


Figure 3: Comparison between the DSL and DSL2 setups.

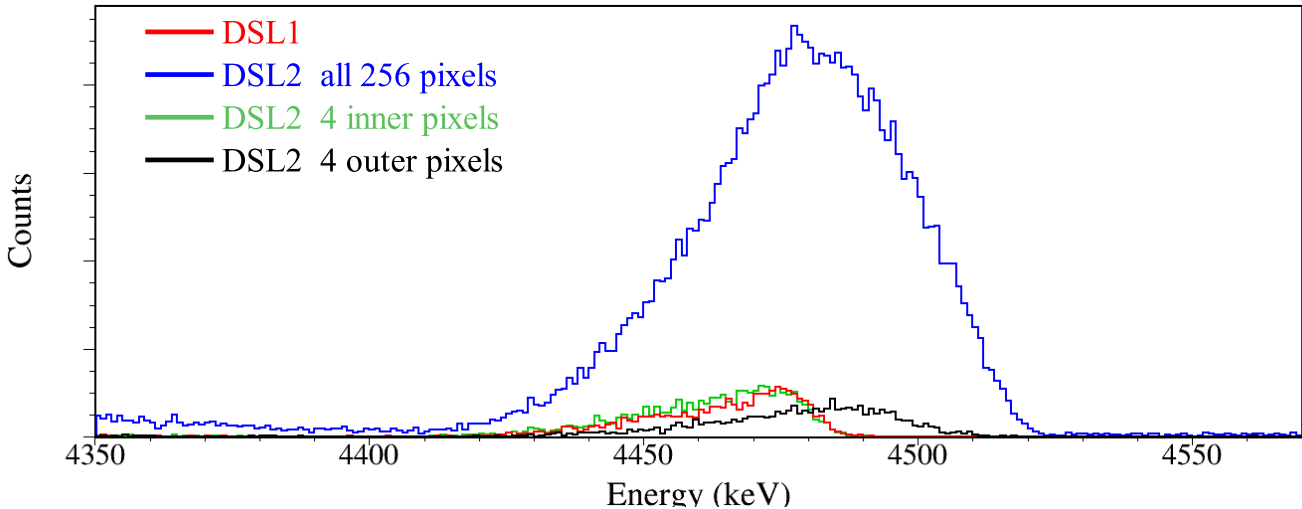


Figure 4: γ -ray spectra for the $6390 \text{ keV} \rightarrow 2234 \text{ keV}$ transition in ^{31}S . The simulation is performed using the DSL1 and DSL2 configuration, respectively, while assuming an equal amount of beam time.

4 Description of the Experiment

The experiment will be conducted using the DSL2 facility [20] at TRIUMF-ISAC-II. A 10 pA , 128-MeV $^{32}\text{S}^{7+}$ beam will bombard a ^3He -implanted Au target and the excited states in ^{31}S will be populated via the $^3\text{He}(^{32}\text{S}, \alpha)^{31}\text{S}$ reaction. The target will be kept cool via BeCu fingers in contact with a BN plate attached to a LN_2 -cooled Cu shroud. The thermal gradient between the target ladder and the Cu shroud prevents losses of the implanted ^3He through heating while mitigating the condensation of contaminants on the surface of the target [25]. The α particles will be detected by the Si detector telescope placed 18.4 mm downstream of the target. The beam and the heavy recoils will be fully stopped inside the $25 \mu\text{m}$ -thick Au foil. Deexcitation γ rays will be detected by a GRIFFIN Ge detector [33, 34] placed at a distance of 78 mm from the target, centered at 0° with respect to the beam axis. The signals from the preamplifiers of the Si and Ge detectors will be collected by the 14-bit, 100-MHz, GRIF-16 digitizers. The data will be processed by the GRIFFIN DAQ [35] and unpacked by the GRSISort program.

The Si detectors will be calibrated using a source containing ^{239}Pu , ^{241}Am , and ^{244}Cm , with strong α lines at 5.155 MeV, 5.486 MeV, and 5.805 MeV. A linear calibration will be applied and used to extrapolate to higher energies. The extrapolation will be verified by comparing the energy loss of punch-through particles to SRIM calculations [36]. The GRIFFIN Ge detector will be calibrated using a ^{56}Co source. A line from ^{197}Au Coulomb excitation at $279.01(5)$ keV [37] and a line from ^{39}K produced in $^{32}\text{S} + ^{12}\text{C}$ fusion evaporation at $2814.06(20)$ keV [38] are usually observed with high statistics. The vast majority of the γ rays constituting these lines were emitted after the recoils stopped; hence, they are unshifted and can be used as run-by-run calibration standards. The accuracy of the calibration at high energies will be verified by a $6128.63(4)$ -keV γ ray originating from the deexcitation of the second excited state in ^{16}O [39]. The energies deposited in all four crystals of the Ge detector will be summed together to increase the photo-peak efficiency while reducing the Compton scattering background [33]. Lifetimes of ^{31}S states will then be determined from a lineshape analysis of this addback spectrum.

After the calibration, we will select α particles with specific energies based on relativistic reaction kinematics, to suppress the competing reaction channels and indirect feedings from higher-lying levels. This approach ensures a direct level population by the transfer reaction, leading to significantly cleaner γ -ray spectra for lineshape analysis. To model the lineshapes in the GEANT4 simulation, the GRIFFIN Ge detector response has to be accurately characterized. We will employ an empirical technique by fitting an exponentially modified Gaussian function [40] to unshifted γ -ray peaks originating from long-lived states

populated by Coulomb excitation and fusion-evaporation reactions at 279.01(5) and 547.5(3) keV [^{197}Au] [37], 2814.06(20) and 3597.26(25) keV [^{39}K] [38], 3736.5(3) keV [^{40}Ca] [41], and 6128.63(4) keV [^{16}O] [39].

5 Readiness

We possess all the equipment needed for the experiment at TRIUMF.

6 Beam Time Required

We acquired \sim 110 hours of data in S1582 using the original DSL setup and observed a total of 51 ± 11 counts in the 4156-keV dominant decay branch of the key ^{31}S resonance at 6390 keV, corresponding to 0.46 counts per hour. Based on the GEANT4 simulation and assuming a beam rate similar to that of S1582, we anticipate 6.6 counts per hour in S2373. This translates to a total of 1020 counts over a period of 152 hours. To investigate the lifetime sensitivity that can be achieved with a factor of 20 increase in statistics, we have generated the same amount of synthetic data for the 4156-keV γ -ray line and incorporated a realistic background level based on our observations in S1582.

The literature energy of the γ ray, the background level beneath the peak, and the stopping power of the target foil have been identified as the most significant factors affecting the lineshapes and, consequently, the inferred lifetime. In the Bayesian framework, the model parameters are viewed as random variables. By varying these parameters within a reasonable range, we first run the GEANT4 simulation with \sim 300 parameter settings (Fig. 5). We have established the analysis framework based on the SURMISE package [44, 45] developed by the Bayesian Analysis for Nuclear Dynamics (BAND) Collaboration [46]. Briefly, we standardize the simulation outputs, extract singular value decomposition to identify principal components, and then project the original simulator outputs onto a lower-dimensional space spanned by an orthogonal basis. This way, the high-dimensional model outputs are transformed into a reduced number of uncorrelated latent outputs using principal component analysis (PCA) [42]. Typically, we set the number of principal components to capture 99.99% of the variance of the model. This means the reduced data set using PCA still retains most of the important information from the original data set. We fit a Gaussian Process (GP) model for each latent output, use the fitted GP model to predict the mean, variance, and covariance matrix, and reconstruct them in the original high-dimensional space through the inverse PCA transformation. When computing the likelihood during MCMC sampling at another parameter setting, the simulator output is represented by the trained emulator's predictive mean and covariance, and the prediction uncertainty from the emulator is integrated within the likelihood. GP is computationally efficient and accurately accounts for the uncertainty associated with emulation, which is suited for Bayesian parameter estimation purposes [43].

The final results obtained from the MCMC sampling are demonstrated in Fig. 6. The lifetime value and its 1σ uncertainties are typically determined by extracting the 16th, 50th, and 84th percentile values from the posterior distribution. In situations where the lifetime falls beyond our sensitivity and is compatible with zero, we can establish its upper limit at a 90% confidence level by using the 90th percentile value from the posterior distribution. One important merit of Bayesian methods is that a posterior distribution offers more detailed information than a point estimate or an interval from frequentist methods so that uncertainty propagation can work with richer information than that conveyed by a point estimate [47, 48]. The 2D correlations between parameters allow us to easily capture features, patterns, or anomalies. The lineshapes based on the prior and posterior distributions of parameters are shown in Fig. 5. The close resemblance between the prediction bands and the measured lineshapes indicates the constraining power provided by the experimental data. With the higher statistics offered by DSL2, it may also be possible to extend the lineshape analysis to other weaker transitions from the resonance to achieve even higher sensitivity on the

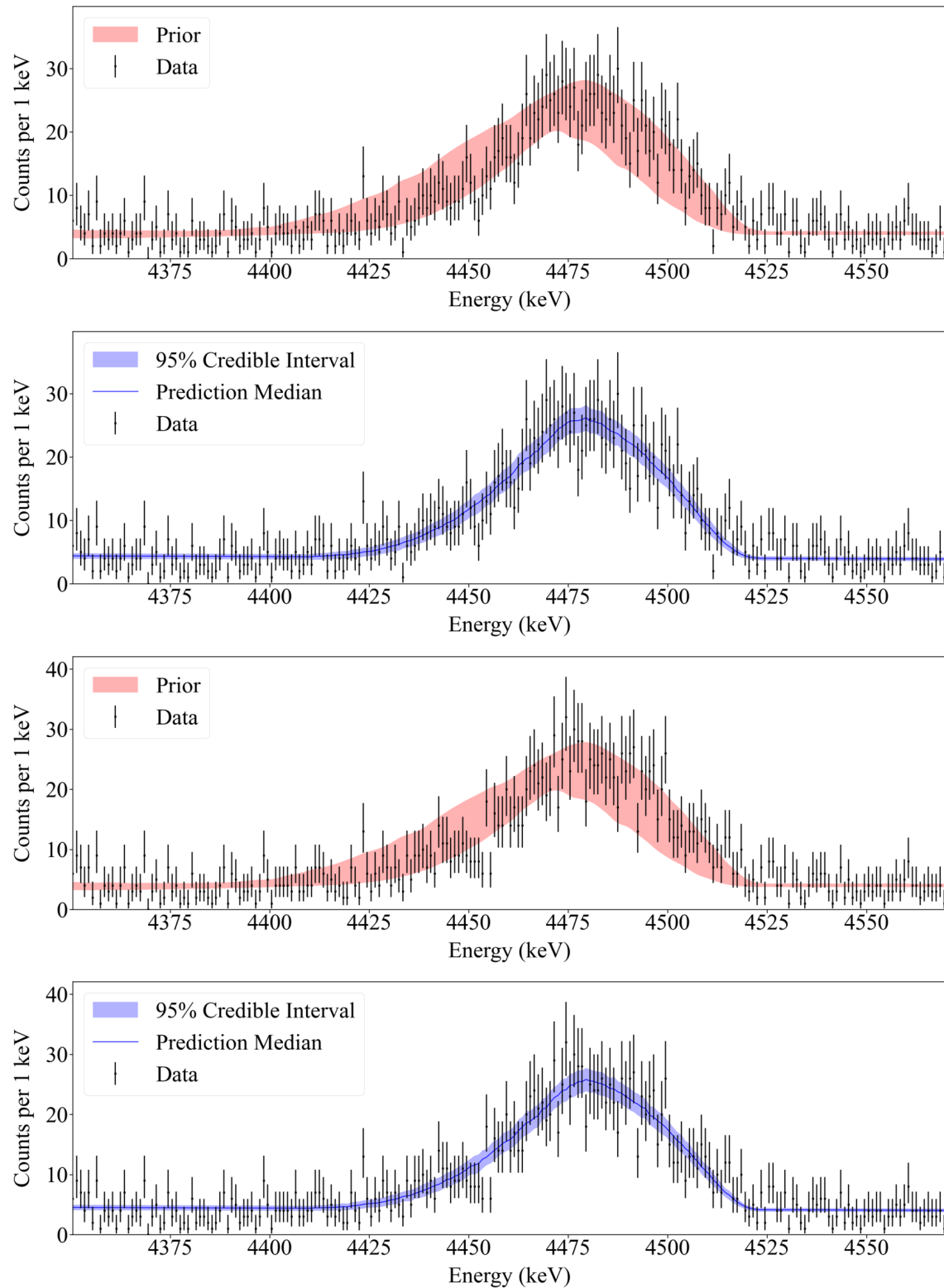


Figure 5: Lineshape analysis of the 4156-keV γ -ray line from the 6390 keV \rightarrow 2234 keV transition in ^{31}S . The lineshapes assuming $\tau = 3$ fs (top two panels) and 0 fs (bottom two panels) are shown as data points with statistical error bars in both panels. Prior lineshape (red, upper panel): hundreds of lineshapes generated by varying each parameter within its prior range in the GEANT4 simulation. Posterior predictive lineshape (blue, lower panel): 95% credible interval constructed with the number of counts in each bin corresponding to the parameter posterior distributions.

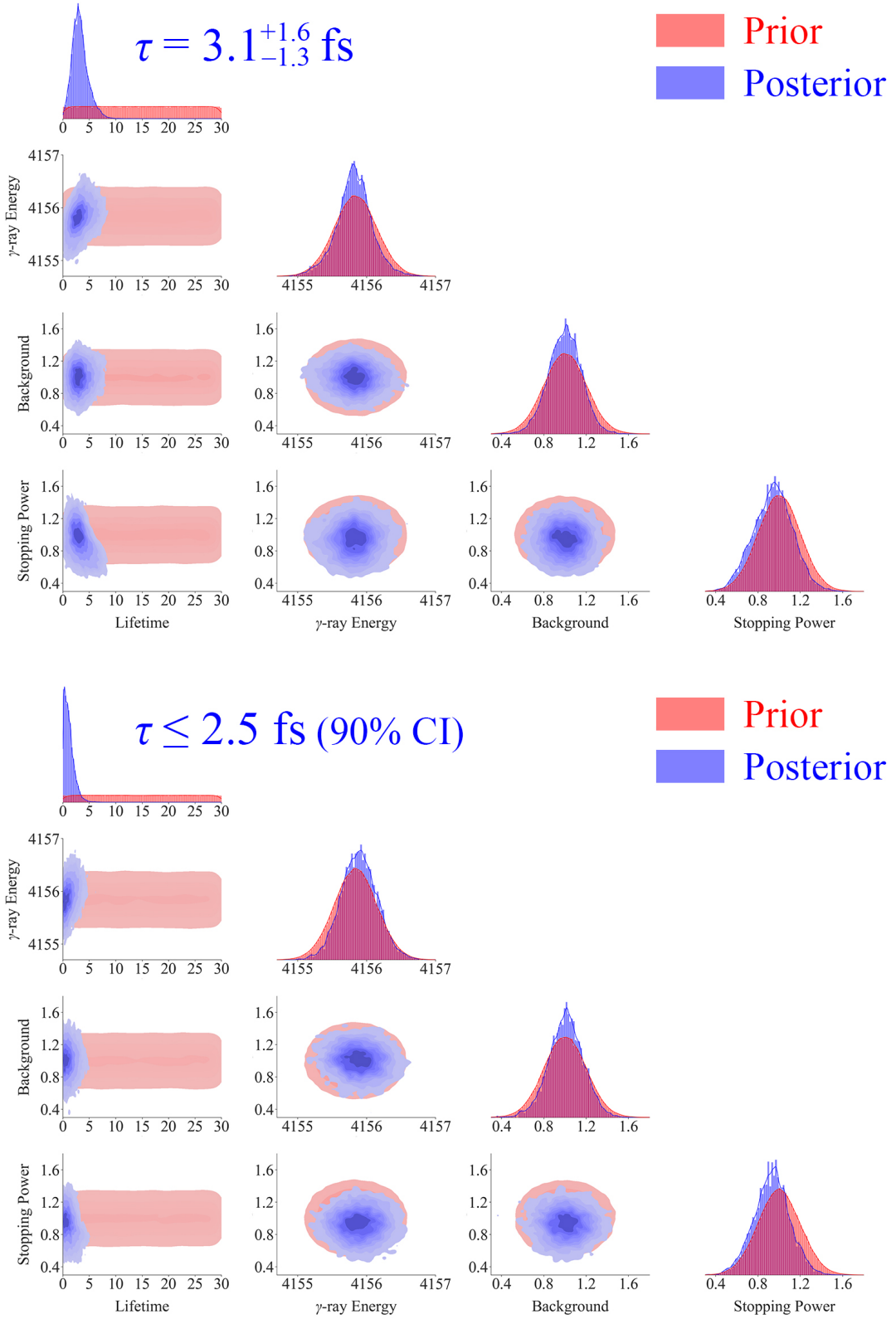


Figure 6: Posterior distributions of the model parameters for the ${}^{31}\text{S}$ $3/2^+$ resonance at 6390 keV assuming a lifetime $\tau = 3$ fs and 0 fs, respectively. Diagonals: prior (red) and posterior (blue) distributions of each parameter. From top left to bottom right: Lifetime τ (fs), γ -ray energy E_γ (keV) of the dominant branch, relative background bkg , and relative stopping power sp . Off-diagonals: joint distributions showing correlations between pairs of parameters.

lifetime, thus facilitating a clearer distinction between the shell-model predictions and contributing to the understanding of the nuclear structure of ^{31}S .

Fig. 7 demonstrates how well we can constrain the resonance strength and the reaction rate with the inferred lifetime. Combining $\tau = 3.1^{+1.6}_{-1.3}$ fs and $\tau \leq 2.5$ fs (90% CI), respectively, with our experimentally determined proton branching ratio $B_p = 2.5^{+0.4}_{-0.3} \times 10^{-4}$ [11] yields resonance strengths $\omega\gamma = 35^{+26}_{-13}$ μeV and $\omega\gamma \geq 43$ μeV (90% CI), respectively. Combining with the well-measured resonance energy $E_r = 259.81(29)$ keV [9], the reaction rate and its uncertainties can be determined without relying on any theoretical assumptions for the first time. Combining with the known properties of other resonances making small contributions within the Gamow window [49, 50, 51, 52, 53, 54, 55], the total thermonuclear $^{30}\text{P}(p, \gamma)^{31}\text{S}$ rate can be determined.

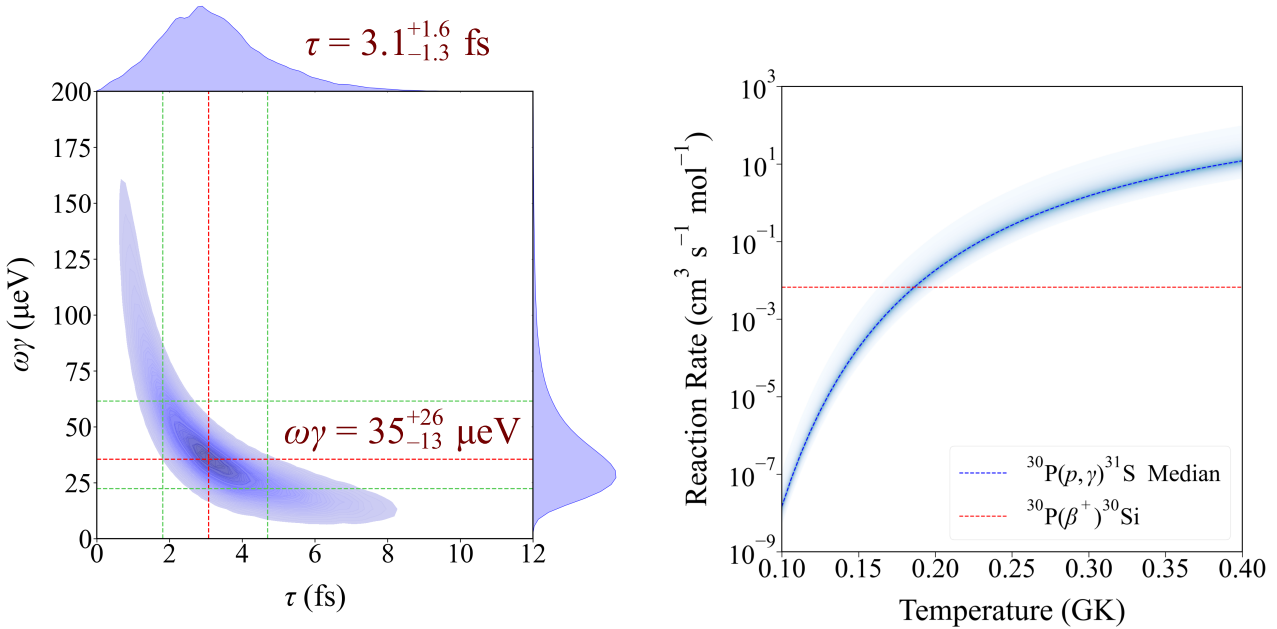


Figure 7: Left: the strength of the 260-keV $3/2^+$ resonance derived from the inferred lifetime of 3 fs and the known proton branching ratio [11]. The resonance strength and its corresponding uncertainties are determined by using the 16th, 50th, and 84th percentile values, which are indicated by dashed lines. Right: the corresponding thermonuclear $^{30}\text{P}(p, \gamma)^{31}\text{S}$ reaction rate from the dominant $3/2^+$ resonance contribution.

To investigate the astrophysical impact, we will perform hydrodynamic simulations of oxygen-neon novae with the spherically symmetric, implicit, Lagrangian, hydrodynamic code SHIVA coupled to a full nuclear reaction network [1, 56]. Briefly, the $^{30}\text{P}(p, \gamma)^{31}\text{S}$ reaction rate and the $^{30}\text{P}(\beta^+)^{30}\text{Si}$ decay are the two main destruction mechanisms for ^{30}P in ONe novae [1]. Fig. 7 shows the proton capture becomes more likely than the competing β^+ decay beyond a temperature within the peak nova temperature range of $T_{\text{peak}} = 0.1\text{--}0.4$ GK. The location of the crossing point influences the predicted Si isotopic ratio for ONe nova ejecta. With the experimentally determined $^{30}\text{P}(p, \gamma)^{31}\text{S}$ rate, we can reach a concrete prediction regarding the presence of ^{30}Si excesses in nova ejecta. This will provide valuable insights into the origin of several presolar grains with significant enhancements in the $^{30}\text{Si}^{28}\text{Si}$ ratio. The elemental abundance ratios of O:S, S:Al, O:P, and P:Al exhibit a strong dependence on both nova temperature and the $^{30}\text{P}(p, \gamma)^{31}\text{S}$ rate. The new rate from this work will allow us to eliminate the dominant nuclear uncertainty and make these ratios more robust nova thermometers.

To summarize, our analysis has demonstrated that with 19 shifts, we can either obtain a finite value as low as 3 fs or set a strong upper limit of 2.5 fs on the lifetime of the astrophysically important $J^\pi = 3/2^+$, 260-keV ${}^{30}\text{P}(p, \gamma){}^{31}\text{S}$ resonance. This level of precision will put the reaction rate on a fully experimental footing for the first time, and will potentially eliminate the largest nuclear uncertainty associated with the aforementioned nova observables. Taking into account an additional 2 shifts of downtime, we request a total of 21 shifts (7 days) to run the experiment.

7 Data analysis

The data analysis will be conducted on the FRIB Lab server, located at Michigan State University, USA.

8 References

1. J. José, *Stellar Explosions: Hydrodynamics and Nucleosynthesis* (CRC/Taylor and Francis: Boca Raton (FL), USA, 2016).
2. C. Iliadis, *Nuclear Physics of Stars* (Wiley-VCH, Verlag, Weinheim, Germany, 2015).
3. J. José, M. Hernanz, and C. Iliadis, *Nucl. Phys. A* **777**, 550 (2006).
4. J. José, M. Hernanz, S. Amari, K. Lodders, and E. Zinner, *Astrophys. J.* **612**, 414 (2004).
5. Lori N. Downen, Christian Iliadis, Jordi José, and Sumner Starrfield, *Astrophys. J.* **762**, 105 (2013).
6. Keegan J. Kelly, Christian Iliadis, Lori Downen, Jordi José, and Art Champagne, *Astrophys. J.* **777**, 130 (2013).
7. C. Wrede, *AIP Advances* **4**, 041004 (2014).
8. M. B. Bennett, C. Wrede, B. A. Brown, S. N. Liddick, D. Pérez-Loureiro, D. W. Bardayan, A. A. Chen, K. A. Chipps, C. Fry, B. E. Glassman, C. Langer, N. R. Larson, E. I. McNeice, Z. Meisel, W. Ong, P. D. O'Malley, S. D. Pain, C. J. Prokop, H. Schatz, S. B. Schwartz, S. Suchyta, P. Thompson, M. Walters, and X. Xu, *Phys. Rev. Lett.* **116**, 102502 (2016).
9. J. Chen, Balraj Singh, *Nucl. Data Sheets* **184**, 29 (2022).
10. M. B. Bennett, C. Wrede, S. N. Liddick, D. Pérez-Loureiro, D. W. Bardayan, B. A. Brown, A. A. Chen, K. A. Chipps, C. Fry, B. E. Glassman, C. Langer, N. R. Larson, E. I. McNeice, Z. Meisel, W. Ong, P. D. O'Malley, S. D. Pain, C. J. Prokop, H. Schatz, S. B. Schwartz, S. Suchyta, P. Thompson, M. Walters, and X. Xu, *Phys. Rev. C* **97**, 065803 (2018).
11. T. Budner, M. Friedman, C. Wrede, B. A. Brown, J. José, D. Pérez-Loureiro, L. J. Sun, J. Surbrook, Y. Ayyad, D. Bardayan, K. Chae, A. Chen, K. Chipps, M. Cortesi, B. Glassman, M. R. Hall, M. Janasik, J. Liang, P. O'Malley, E. Pollacco, A. Psaltis, J. Stomps, and T. Wheeler, *Phys. Rev. Lett.* **128**, 182701 (2022).
12. R. Engmann, E. Ehrmann, F. Brandolini, and C. Signorini, *Nucl. Phys. A* **162**, 295 (1971).
13. P. Doornenbal, P. Reiter, H. Grawe, T. Saito, A. Al-Khatib, A. Banu, T. Beck, F. Becker, P. Bednarczyk, G. Benzoni, A. Bracco, A. Bürger, L. Caceres, F. Camera, S. Chmel, F.C.L. Crespi, H. Geissel, J. Gerl, M. Górska, J. Grebosz, H. Hübel, M. Kavatsyuk, O. Kavatsyuk, M. Kmiecik, I. Kojouharov, N. Kurz, R. Lozeva, A. Maj, S. Mandal, W. Meczynski, B. Million, Zs. Podolyák, A. Richard, N. Saito, H. Schaffner, M. Seidlitz, T. Striepling, J. Walker, N. Warr, H. Weick, O. Wieland, M. Winkler, and H.J. Wollersheim, *Nucl. Instrum. Methods Phys. Res. A* **613**, 218 (2010).
14. Clemens Herlitzius, *Ph.D. Thesis*, Technische Universität München, Germany, 2013.
15. D. Tonev, G. de Angelis, I. Deloncle, N. Goutev, G. De Gregorio, P. Pavlov, I.L. Pantaleev, S. Iliev, M.S. Yavahchova, P.G. Bizzeti, A. Demerdjiev, D.T. Dimitrov, E. Farnea, A. Gadea, E. Geleva, C.Y. He, H. Laftchiev, S.M. Lenzi, S. Lunardi, N. Marginean, R. Menegazzo, D.R. Napoli, F. Nowacki, R. Orlandi, H. Penttilä, F. Recchia, E. Sahin, R.P. Singh, M. Stoyanova, C.A. Ur, H.-F. Wirth, *Phys. Lett. B* **821**, 136603 (2021).
16. N. S. Pattabiraman, D. G. Jenkins, M. A. Bentley, R. Wadsworth, C. J. Lister, M. P. Carpenter, R. V. F. Janssens, T. L. Khoo, T. Lauritsen, D. Seweryniak, S. Zhu, G. Lotay, P. J. Woods, Krishchayan, and P. Van Isacker, *Phys. Rev. C* **78**, 024301 (2008).
17. Tamas Budner, *Ph.D. Thesis*, Michigan State University, Michigan, USA, 2022.
18. L. J. Sun, C. Fry, B. Davids, N. Esker, C. Wrede, M. Alcorta, S. Bhattacharjee, M. Bowry, B. A. Brown, T. Budner, R. Caballero-Folch, L. Evitts, M. Friedman, A. B. Garnsworthy, B. E. Glassman, G. Hackman, J. Henderson, O. S. Kirsebom, J. Lighthall, P. Machule, J. Measures, M. Moukaddam, J. Park, C. Pearson, D.

- Pérez-Loureiro, C. Ruiz, P. Ruotsalainen, J. Smallcombe, J. K. Smith, D. Southall, J. Surbrook, L. E. Weghorn, and M. Williams, [Phys. Lett. B 839, 137801 \(2023\)](#).
19. Alex Brown, private communication.
 20. B. Davids, [Hyperfine Interact. 225, 215 \(2014\)](#).
 21. R. Kanungo, T. K. Alexander, A. N. Andreyev, G. C. Ball, R. S. Chakrawarthy, M. Chicoine, R. Churchman, B. Davids, J. S. Forster, S. Gujrathi, G. Hackman, D. Howell, J. R. Leslie, A. C. Morton, S. Mythili, C. J. Pearson, J. J. Ressler, C. Ruiz, H. Savajols, M. A. Schumaker, I. Tanihata, P. Walden, and S. Yen, [Phys. Rev. C 74, 045803 \(2006\)](#).
 22. S. Mythili, B. Davids, T. K. Alexander, G. C. Ball, M. Chicoine, R. S. Chakrawarthy, R. Churchman, J. S. Forster, S. Gujrathi, G. Hackman, D. Howell, R. Kanungo, J. R. Leslie, E. Padilla, C. J. Pearson, C. Ruiz, G. Ruprecht, M. A. Schumaker, I. Tanihata, C. Vockenhuber, P. Walden, and S. Yen, [Phys. Rev. C 77, 035803 \(2008\)](#).
 23. N. Galinski, S. K. L. Sjue, G. C. Ball, D. S. Cross, B. Davids, H. Al Falou, A. B. Garnsworthy, G. Hackman, U. Hager, D. A. Howell, M. Jones, R. Kanungo, R. Kshetri, K. G. Leach, J. R. Leslie, M. Moukaddam, J. N. Orce, E. T. Rand, C. Ruiz, G. Ruprecht, M. A. Schumaker, C. E. Svensson, S. Triambak, and C. D. Unsworth, [Phys. Rev. C 90, 035803 \(2014\)](#).
 24. O. S. Kirsebom, P. Bender, A. Cheeseman, G. Christian, R. Churchman, D. S. Cross, B. Davids, L. J. Evitts, J. Fallis, N. Galinski, A. B. Garnsworthy, G. Hackman, J. Lighthall, S. Ketelhut, P. Machule, D. Miller, S. T. Nielsen, C. R. Nobs, C. J. Pearson, M. M. Rajabali, A. J. Radich, A. Rojas, C. Ruiz, A. Sanetullaev, C. D. Unsworth, and C. Wrede, [Phys. Rev. C 93, 025802 \(2016\)](#).
 25. Cathleen Fry, Ph.D. Thesis, Michigan State University, Michigan, USA, 2018.
 26. ORTEC B Series Totally Depleted Silicon Surface Barrier Radiation Detector.
 27. MIRCON W1 Double-sided Silicon Strip Detector.
 28. MIRCON MSX25 Single-side Large Area Silicon Detector.
 29. S. Agostinelli, J. Allison, K. Amako, J. Apostolakis, H. Araujo, P. Arce, M. Asai, D. Axen, S. Banerjee, G. Barrand, F. Behner, L. Bellagamba, J. Boudreau, L. Broglia, A. Brunengo, H. Burkhardt, S. Chauvie, J. Chuma, R. Chytracek, G. Cooperman, G. Cosmo, P. Degtyarenko, A. Dell'Acqua, G. Depaola, D. Dietrich, R. Enami, A. Feliciello, C. Ferguson, H. Fesefeldt, G. Folger, F. Foppiano, A. Forti, S. Garelli, S. Giani, R. Giannitrapani, D. Gibin, J. J. Gómez Cadenas, I. González, G. Gracia Abril, G. Greeniaus, W. Greiner, V. Grichine, A. Grossheim, S. Guatelli, P. Gumplinger, R. Hamatsu, K. Hashimoto, H. Hasui, A. Heikkinen, A. Howard, V. Ivanchenko, A. Johnson, F. W. Jones, J. Kallenbach, N. Kanaya, M. Kawabata, Y. Kawabata, M. Kawaguti, S. Kelner, P. Kent, A. Kimura, T. Kodama, R. Kokoulin, M. Kossov, H. Kurashige, E. Lamanna, T. Lampén, V. Lara, V. Lefebure, F. Lei, M. Liendl, W. Lockman, F. Longo, S. Magni, M. Maire, E. Medernach, K. Minamimoto, P. Mora de Freitas, Y. Morita, K. Murakami, M. Nagamatu, R. Nartallo, P. Nieminen, T. Nishimura, K. Ohtsubo, M. Okamura, S. O'Neale, Y. Oohata, K. Paech, J. Perl, A. Pfeiffer, M. G. Pia, F. Ranjard, A. Rybin, S. Sadilov, E. Di Salvo, G. Santin, T. Sasaki, N. Savvas, Y. Sawada, S. Scherer, S. Sei, V. Sirotenko, D. Smith, N. Starkov, H. Stoecker, J. Sulkimo, M. Takahata, S. Tanaka, E. Tcherniaev, E. Safai Tehrani, M. Tropeano, P. Truscott, H. Uno, L. Urban, P. Urban, M. Verderi, A. Walkden, W. Wander, H. Weber, J. P. Wellisch, T. Wenaus, D. C. Williams, D. Wright, T. Yamada, H. Yoshida, and D. Zschiesche, [Nucl. Instrum. Methods Phys. Res. A 506, 250 \(2003\)](#).
 30. J. Allison, K. Amako, J. Apostolakis, P. Arce, M. Asai, T. Aso, E. Bagli, A. Bagulya, S. Banerjee, G. Barrand, B.R. Beck, A.G. Bogdanov, D. Brandt, J.M.C. Brown, H. Burkhardt, Ph. Canal, D. Cano-Ott, S. Chauvie, K. Cho, G.A.P. Cirrone, G. Cooperman, M.A. Cortés-Giraldo, G. Cosmo, G. Cuttone, G. Depaola, L. Desorgher, X. Dong, A. Dotti, V.D. Elvira, G. Folger, Z. Francis, A. Galoyan, L. Garnier, M. Gayer, K.L. Genser, V.M. Grichine, S. Guatelli, P. Guèye, P. Gumplinger, A.S. Howard, I. Hřivnáčová, S. Hwang, S. Incerti, A. Ivanchenko, V.N. Ivanchenko, F.W. Jones, S.Y. Jun, P. Kaitaniemi, N. Karakatsanis, M. Karamitros, M. Kelsey, A. Kimura, T. Koi, H. Kurashige, A. Lechner, S.B. Lee, F. Longo, M. Maire, D. Mancusi, A. Mantero, E. Mendoza, B. Morgan, K. Murakami, T. Nikitina, L. Pandola, P. Paprocki, J. Perl, I. Petrović, M.G. Pia, W. Pokorski, J.M. Quesada, M. Raine, M.A. Reis, A. Ribon, A. Ristić Fira, F. Romano, G. Russo, G. Santin, T. Sasaki, D. Sawkey, J.I. Shin, I.I. Strakovský, A. Taborda, S. Tanaka, B. Tomé, T. Toshito, H.N. Tran, P.R. Truscott, L. Urban, V. Uzhinsky, J.M. Verbeke, M. Verderi, B.L. Wendt, H. Wenzel, D.H. Wright, D.M. Wright, T. Yamashita, J. Yarba, H. Yoshida, [Nucl. Instrum. Methods Phys. Res. A 835, 186 \(2016\)](#).
 31. TRIUMF S2193: Lifetime of the key $^{22}\text{Na}(p, \gamma)^{23}\text{Mg}$ resonance in novae.
 32. Lexanne Weghorn, Ph.D. Thesis in progress, Michigan State University, Michigan, USA.
 33. U. Rizwan, A. B. Garnsworthy, C. Andreou, G. C. Ball, A. Chester, T. Domingo, R. Dunlop, G. Hackman, E. T. Rand, J. K. Smith, K. Starosta, C. E. Svensson, P. Voss, and J. Williams, [Nucl. Instrum. Methods Phys.](#)

Res. A **820**, 126 (2016).

34. A.B. Garnsworthy, C.E. Svensson, M. Bowry, R. Dunlop, A.D. MacLean, B. Olaizola, J.K. Smith, F.A. Ali, C. Andreoiu, J.E. Ash, W.H. Ashfield, G.C. Ball, T. Ballast, C. Bartlett, Z. Beadle, P.C. Bender, N. Bernier, S.S. Bhattacharjee, H. Bidaman, V. Bildstein, D. Bishop, P. Boubel, R. Braid, D. Brennan, T. Bruhn, C. Burbadge, A. Cheeseman, A. Chester, R. Churchman, S. Ciccone, R. Caballero-Folch, D.S. Cross, S. Cruz, B. Davids, A. Diaz Varela, I. Dillmann, M.R. Dunlop, L.J. Evitts, F.H. Garcia, P.E. Garrett, S. Georges, S. Gillespie, R. Gudapati, G. Hackman, B. Hadinia, S. Hallam, J. Henderson, S.V. Ilyushkin, B. Jigmeddorj, A.I. Kilic, D. Kisliuk, R. Kokke, K. Kuhn, R. Krücke, M. Kuwabara, A.T. Laffoley, R. Lafleur, K.G. Leach, J.R. Leslie, Y. Linn, C. Lim, E. MacConnachie, A.R. Mathews, E. McGee, J. Measures, D. Miller, W.J. Mills, W. Moore, D. Morris, L.N. Morrison, M. Moukaddam, C.R. Natzke, K. Ortner, E. Padilla-Rodal, O. Paetkau, J. Park, H.P. Patel, C.J. Pearson, E. Peters, E.E. Peters, J.L. Pore, A.J. Radich, M.M. Rajabali, E.T. Rand, K. Raymond, U. Rizwan, P. Ruotsalainen, Y. Saito, F. Sarazin, B. Shaw, J. Smallcombe, D. Southall, K. Starosta, M. Ticu, E. Timakova, J. Turko, R. Umashankar, C. Unsworth, Z.M. Wang, K. Whitmore, S. Wong, S.W. Yates, E.F. Zganjar, and T. Zidar, *Nucl. Instrum. Methods Phys. Res. A* **918**, 9 (2019).
35. A.B. Garnsworthy, C.J. Pearson, D. Bishop, B. Shaw, J.K. Smith, M. Bowry, V. Bildstein, G. Hackman, P.E. Garrett, Y. Linn, J.-P. Martin, W.J. Mills, C.E. Svensson, *Nucl. Instrum. Methods Phys. Res. A* **853**, 85 (2017).
36. J. F. Ziegler, M. D. Ziegler, and J. P. Biersack, *Nucl. Instrum. Methods Phys. Res. B* **268**, 1818 (2010).
37. Xiaolong Huang and Chunmei Zhou, *Nucl. Data Sheets* **104**, 283 (2005).
38. J. Chen, *Nucl. Data Sheets* **149**, 1 (2018).
39. D.R. Tilley, H.R. Weller, and C.M. Cheves, *Nucl. Phys. A* **564**, 1 (1993).
40. L. J. Sun, M. Friedman, T. Budner, D. Pérez-Loureiro, E. Pollacco, C. Wrede, B. A. Brown, M. Cortesi, C. Fry, B. E. Glassman, J. Heideman, M. Janasik, A. Kruskie, A. Magilligan, M. Roosa, J. Stomps, J. Surbrook, and P. Tiwari, *Phys. Rev. C* **103**, 014322 (2021).
41. J. Chen, *Nucl. Data Sheets* **140**, 1 (2017).
42. Michael E. Tipping and Christopher M. Bishop, *Neural Comput.* **11**, 443 (1999).
43. C. E. Rasmussen and C. K. I. Williams, *Gaussian Processes for Machine Learning* (Cambridge, MA: The MIT Press, 2006).
44. Ö. Sürer, F. M. Nunes, M. Plumlee, and S. M. Wild, *Phys. Rev. C* **106**, 024607 (2022).
45. SURMISE package.
46. D. R. Phillips, R. J. Furnstahl, U. Heinz, T. Maiti, W. Nazarewicz, F. M. Nunes, M. Plumlee, M. T. Pratola, S. Pratt, F. G. Viens, and S. M. Wild, *J. Phys. G: Nucl. Part. Phys.* **48**, 072001 (2021).
47. Sanjib Sharma, *Annu. Rev. Astron. Astrophys.* **55**, 213 (2017).
48. Evaluation of measurement data - Supplement 1 to the *Guide to the expression of uncertainty in measurement - Propagation of distributions using a Monte Carlo method*. Joint Committee for Guides in Metrology, **101**, 2008.
49. D. T. Doherty, G. Lotay, P. J. Woods, D. Seweryniak, M. P. Carpenter, C. J. Chiara, H. M. David, R. V. F. Janssens, L. Trache, and S. Zhu, *Phys. Rev. C* **108**, 262502 (2012).
50. D. T. Doherty, P. J. Woods, G. Lotay, D. Seweryniak, M. P. Carpenter, C. J. Chiara, H. M. David, R. V. F. Janssens, L. Trache, and S. Zhu, *Phys. Rev. C* **89**, 045804 (2014).
51. A. Kankainen, P.J. Woods, H. Schatz, T. Poxon-Pearson, D.T. Doherty, V. Bader, T. Baugher, D. Bazin, B.A. Brown, J. Browne, A. Estrade, A. Gade, J. José, A. Kontos, C. Langer, G. Lotay, Z. Meisel, F. Montes, S. Noji, F. Nunes, G. Perdikakis, J. Pereira, F. Recchia, T. Redpath, R. Stroberg, M. Scott, D. Seweryniak, J. Stevens, D. Weisshaar, K. Wimmer, R. Zegers, *Phys. Lett. B* **769**, 549 (2017).
52. D. G. Jenkins, C. J. Lister, M. P. Carpenter, P. Chowdhury, N. J. Hammond, R. V. F. Janssens, T. L. Khoo, T. Lauritsen, D. Seweryniak, T. Davinson, P. J. Woods, A. Jokinen, and H. Penttila, *Phys. Rev. C* **72**, 031303(R) (2005).
53. D. G. Jenkins, A. Meadowcroft, C. J. Lister, M. P. Carpenter, P. Chowdhury, N. J. Hammond, R. V. F. Janssens, T. L. Khoo, T. Lauritsen, D. Seweryniak, T. Davinson, P. J. Woods, A. Jokinen, H. Penttila, G. Martínez-Pinedo, and J. José, *Phys. Rev. C* **89**, 045804 (2014).
54. D. A. Testov, A. Bosso, S. M. Lenzi, F. Nowacki, F. Recchia, G. de Angelis, D. Bazzacco, G. Colucci, M. Cottini, F. Galtarossa, A. Goasduff, A. Gozzelino, K. Hadyńska-Klek, G. Jaworski, P. R. John, S. Lunardi, R. Menegazzo, D. Mengoni, A. Mentana, V. Modamio, A. Nannini, D. R. Napoli, M. Palacz, M. Rocchini, M. Siciliano, and J. J. Valiente-Dobón, *Phys. Rev. C* **104**, 024309 (2021).
55. K. Setodehnia, A. A. Chen, J. Chen, J. A. Clark, C. M. Deibel, J. Hendriks, D. Kahl, W. N. Lennard, P. D. Parker, D. Seiler, and C. Wrede, *Phys. Rev. C* **102**, 045806 (2020).
56. J. José and M. Hernanz, *Astrophys. J* **494**, 680 (1998).